

The Mode III Crack Problem in Microstructured Solids Governed by Dipolar Gradient Elasticity: Static and Dynamic Analysis

H. G. Georgiadis

Mechanics Division,
National Technical University of Athens,
1 Konitsis Street,
Zographou GR-15773, Greece
e-mail: georgiad@central.ntua.gr
Mem. ASME

This study aims at determining the elastic stress and displacement fields around a crack in a microstructured body under a remotely applied loading of the antiplane shear (mode III) type. The material microstructure is modeled through the Mindlin-Green-Rivlin dipolar gradient theory (or strain-gradient theory of grade two). A simple but yet rigorous version of this generalized continuum theory is taken here by considering an isotropic linear expression of the elastic strain-energy density in antiplane shearing that involves only two material constants (the shear modulus and the so-called gradient coefficient). In particular, the strain-energy density function, besides its dependence upon the standard strain terms, depends also on strain gradients. This expression derives from form II of Mindlin's theory, a form that is appropriate for a gradient formulation with no couple-stress effects (in this case the strain-energy density function does not contain any rotation gradients). Here, both the formulation of the problem and the solution method are exact and lead to results for the near-tip field showing significant departure from the predictions of the classical fracture mechanics. In view of these results, it seems that the conventional fracture mechanics is inadequate to analyze crack problems in microstructured materials. Indeed, the present results suggest that the stress distribution ahead of the tip exhibits a local maximum that is bounded. Therefore, this maximum value may serve as a measure of the critical stress level at which further advancement of the crack may occur. Also, in the vicinity of the crack tip, the crack-face displacement closes more smoothly as compared to the classical results. The latter can be explained physically since materials with microstructure behave in a more rigid way (having increased stiffness) as compared to materials without microstructure (i.e., materials governed by classical continuum mechanics). The new formulation of the crack problem required also new extended definitions for the J-integral and the energy release rate. It is shown that these quantities can be determined through the use of distribution (generalized function) theory. The boundary value problem was attacked by both the asymptotic Williams technique and the exact Wiener-Hopf technique. Both static and time-harmonic dynamic analyses are provided. [DOI: 10.1115/1.1574061]

1 Introduction

The present work is concerned with the exact determination of mode III crack-tip fields within the framework of the dipolar gradient elasticity (or strain-gradient elasticity of grade two). This theory was introduced by Mindlin [1], Green and Rivlin [2], and Green [3] in an effort to model the mechanical response of materials with *microstructure*. The theory begins with the very general concept of a continuum containing elements or particles (called macromedia), which are in themselves *deformable* media. This behavior can easily be realized if such a macro-particle is viewed as a collection of smaller subparticles (called micromedia). In this way, each particle of the continuum is endowed with an *internal* displacement field, which is expanded as a power series in internal coordinate variables. Within the above context, the lowest-order theory (dipolar or grade-two theory) is the one obtained by retaining only the first (linear) term. Also, since these theories introduce

dependence on strain and/or rotation gradients, the new material constants imply the presence of characteristic lengths in the material behavior, which allow the incorporation of size effects into stress analysis in a manner that the classical theory cannot afford.

The Mindlin-Green-Rivlin theory and related ideas, after a first development and some successful applications mainly on stress concentration problems during the sixties (see, e.g., Mindlin and Eshel [4], Weitsman [5], Day and Weitsman [6], Cook and Weitsman [7], Herrmann and Achenbach [8], and Achenbach et al. [9]), have also recently been employed to analyze complex problems in materials with microstructure (see, e.g., Vardoulakis and Sulem [10], Fleck et al. [11], Lakes [12], Vardoulakis and Georgiadis [13], Wei and Huthinson [14], Begley and Huthinson [15], Exadaktylos and Vardoulakis [16], Huang et al. [17], Zhang et al. [18], Chen et al. [19], Georgiadis and Vardoulakis [20], Georgiadis et al. [21,22], Georgiadis and Velgaki [23], and Amanatidou and Aravas [24]). More specifically, recent work by the author and co-workers [13,20–23], on wave-propagation problems showed that the gradient approach predicts types of elastic waves that are not predicted by the classical theory (SH and torsional *surface* waves in homogeneous materials) and also predicts *dispersion* of high-frequency Rayleigh waves (the classical elasticity fails to predict dispersion of these waves at *any* frequency). Notice that all these phenomena are observed in experiments and are also predicted by atomic-lattice analyses (see, e.g., Gazis et al. [25]).

Contributed by the Applied Mechanics Division of THE AMERICAN SOCIETY OF MECHANICAL ENGINEERS for publication in the ASME JOURNAL OF APPLIED MECHANICS. Manuscript received by the ASME Applied Mechanics Division, Apr. 28, 2002; final revision, Dec. 19, 2002. Associate Editor: B. M. Moran. Discussion on the paper should be addressed to the Editor, Prof. Robert M. McMeeking, Department of Mechanical and Environmental Engineering University of California—Santa Barbara, Santa Barbara, CA 93106-5070, and will be accepted until four months after final publication of the paper itself in the ASME JOURNAL OF APPLIED MECHANICS.

Thus, based on existing gradient-type results, one may conclude that the Mindlin-Green-Rivlin theory extends the range of applicability of continuum theories in an effort towards bridging the gap between classical (monopolar or nongeneralized) theories of continua and theories of atomic lattices.

In the present work the concept adopted, following the aforementioned ideas, is to view the continuum as a periodic structure like that, e.g., of crystal lattices, crystallites of a polycrystal or grains of a granular material. The material is composed wholly of unit cells (micromedia) having the form of cubes with edges of size $2h$. This size is therefore an intrinsic material length. We further assume (and this is a rather standard assumption in studies applying the Mindlin-Green-Rivlin theory to practical problems) that the continuum is *homogeneous* in the sense that the relative deformation (i.e., the difference between the macrodisplacement gradient and the microdeformation—cf. Mindlin [1]) is zero and the microdensity does not differ from the macrodensity. Then, we formulate the mode III crack problem by considering an isotropic and linear expression of the strain-energy density W . This expression in antiplane shear and with respect to a Cartesian coordinate system $Ox_1x_2x_3$ reads $W = \mu \varepsilon_{p3} \varepsilon_{p3} + \mu c (\partial_s \varepsilon_{p3}) (\partial_s \varepsilon_{p3})$, where the summation convention is understood over the Latin indices, which take the values 1 and 2 only, $(\varepsilon_{13}, \varepsilon_{23})$ are the only identically nonvanishing components of the linear strain tensor, μ is the shear modulus, c is the gradient coefficient (a positive constant accounting for microstructural effects), and $\partial_s(\cdot) \equiv \partial(\cdot)/\partial x_s$. The problem is two-dimensional and is stated in the plane (x_1, x_2) . The above strain-energy density function is the simplest possible form of case II in Mindlin's [1] theory and is appropriate for a gradient formulation with *no* couple-stress effects, because W is completely *independent* upon rotation gradients. Indeed, by referring to a strain-energy density function that depends upon strains and strain gradients in a three-dimensional body (the Latin indices now span the range (1,2,3)), i.e., a function of the form $W = (1/2)c_{pqsj} \varepsilon_{pq} \varepsilon_{sj} + (1/2)d_{pqsjlm} \kappa_{pq} \kappa_{jlm}$ with (c_{pqsj}, d_{pqsjlm}) being tensors of material constants and $\kappa_{pq} = \partial_p \varepsilon_{qs} \equiv \partial_p \varepsilon_{sq}$, and by defining the Cauchy (in Mindlin's notation) stress tensor as $\tau_{pq} = \partial W / \partial \varepsilon_{pq}$ and the dipolar stress tensor (a third-rank tensor) as $m_{pq} = \partial W / \partial (\partial_p \varepsilon_{qs})$, one may observe that the relations $m_{pq} = m_{p(qs)}$ and $m_{[qs]} = 0$ hold, where (\cdot) and $[\cdot]$ as subscripts denote the symmetric and antisymmetric parts of a tensor, respectively. Accordingly, couple stresses do not appear within the present formulation by assuming dipolar (internal) forces with vanishing antisymmetric part (more details on this are given in Section 2 below). A couple-stress, quasi-static solution of the mode-III crack problem was given earlier by Zhang et al. [18]. Note in passing that in the literature one may find mainly two types of approaches: In the first type (couple-stress case) the strain-energy density depends on rotation gradients and has no dependence upon strain gradients of the kind mentioned above (see, e.g., [11,17–19,23]), whereas in the second type the strain-energy density depends on strain gradients and has no dependence upon rotation gradients (see, e.g., [13,16,20–22]). Exceptions from this trend exist of course (see, e.g., [5–7]) and these works employ a more complicated formulation based on form III of Mindlin's theory, [1].

Here, in addition to the quasi-static case, we also treat the time-harmonic dynamical case, which is pertinent to the problem of stress-wave diffraction by a pre-existing crack in the body. In the latter case, besides the standard inertia term in the equation of motion, a micro-inertia term is also taken into account (in a consistent and rigorous manner by considering the proper kinetic-energy density) and this leads to an *explicit* appearance of the intrinsic material length h . We emphasize that quasi-static approaches cannot include explicitly the size of the material cell in their governing equations. In these approaches, rather, a characteristic length appears in the governing equations only through the gradient coefficient c (which has dimensions of $[\text{length}]^2$) in the gradient theory without couple-stress effects or the ratio (η/μ)

(which again has dimensions of $[\text{length}]^2$) in the couple-stress theory without the effects of collinear dipolar forces, where η is the couple-stress modulus and μ is the shear modulus of the material. Of course, one of the quantities c or (η/μ) also appears within a dynamic analysis, which therefore may allow for an interrelation of the two different characteristic lengths (the one introduced in the strain energy and the other introduced in the kinetic energy—see relative works by Georgiadis et al. [22] and Georgiadis and Velgaki [23]). Indeed, by comparing the forms of dispersion curves of Rayleigh waves obtained by the dipolar (“pure” gradient and couple-stress) approaches with the ones obtained by the atomic-lattice analysis of Gazis et al. [25], it can be estimated that c is of the order of $(0.1h)^2$, [22], and η is of the order of $0.1\mu h^2$, [23].

The mathematical analysis of the dynamical problem here presents some novel features related to the Wiener-Hopf technique not encountered in dealing with the static case. The Wiener-Hopf technique is employed to obtain exact solutions in both cases, and also the Williams technique is employed for an asymptotic determination of the near-tip fields. Also, since the gradient formulation exhibits a *singular-perturbation* character, the concept of a *boundary layer* is employed to accomplish the solution. On the other hand, the gradient formulation demands extended definitions of the J -integral and the energy release rate. It is further proved, by utilizing some theorems of distribution theory, that both energy quantities remain bounded despite the hypersingular behavior of the near-tip stress field. Finally, physical aspects of the solution are discussed with particular reference to the closure of the crack faces and the nature of cohesive tractions.

2 Fundamentals of the Dipolar Gradient Elasticity

A brief account of the Mindlin-Green-Rivlin theory, [1–3], pertaining to the elastodynamics of homogeneous and isotropic materials is given here. If a continuum with microstructure is viewed as a collection of subparticles (micromedia) having the form of unit cells (cubes), the following expression of the kinetic-energy density (kinetic energy per unit macrovolume) is obtained with respect to a Cartesian coordinate system $Ox_1x_2x_3$, [1],

$$T = \frac{1}{2} \rho \dot{u}_p \dot{u}_p + \frac{1}{6} \rho h^2 (\partial_p \dot{u}_q) (\partial_p \dot{u}_q), \quad (1)$$

where ρ is the mass density, $2h$ is the size of the cube edges, u_p is the displacement vector, $\partial_p(\cdot) \equiv \partial(\cdot)/\partial x_p$, $(\dot{\cdot}) \equiv \partial(\cdot)/\partial t$ with t denoting the time, and the Latin indices span the range (1,2,3). We also notice that Georgiadis et al. [22] by using the concept of *internal* motions have obtained (1) in an alternative way to that by Mindlin [1]. In the RHS of Eq. (1), the second term representing the effects of velocity gradients (a term not encountered within classical continuum mechanics) reflects the greater detail with which the dipolar theory describes the motion.

Next, the following expression of the strain-energy density is postulated:

$$W = \frac{1}{2} c_{pqsj} \varepsilon_{pq} \varepsilon_{sj} + \frac{1}{2} d_{pqsjlm} \kappa_{pq} \kappa_{jlm}, \quad (2)$$

where (c_{pqsj}, d_{pqsjlm}) are tensors of material constants, $\varepsilon_{pq} = (1/2)(\partial_p u_q + \partial_q u_p)$ is the linear strain tensor, and $\kappa_{pq} = \partial_p \varepsilon_{qs}$ is the strain gradient. Notice that in the tensors c_{pqsj} and d_{pqsjlm} (which are of even rank) the number of independent components can be reduced to yield isotropic constitutive relations. Such an isotropic behavior is considered here. Again, the form in (2) can be viewed as a more accurate description of the constitutive response than that provided by the classical elasticity, if one thinks of a series expansion for W containing higher-order strain gradients. Also, one may expect that the additional term (or terms) will be significant in the vicinity of stress-concentration points where the strain undergoes very steep variations.

Then, pertinent stress tensors can be defined by taking the variation of W

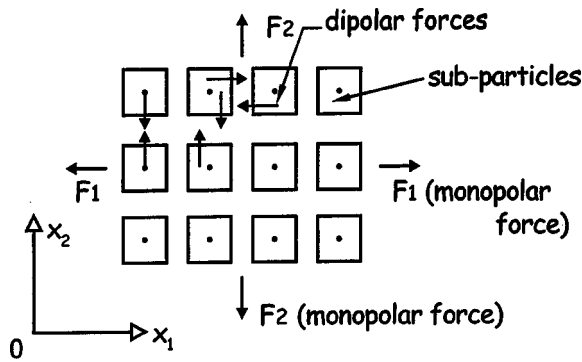


Fig. 1 Monopolar (external) and dipolar (internal) forces acting on an ensemble of subparticles in a material with micro-structure

$$\tau_{pq} = \frac{\partial W}{\partial \varepsilon_{pq}}, \quad (3a)$$

$$m_{pqs} = \frac{\partial W}{\partial \kappa_{pqs}} \equiv \frac{\partial W}{\partial (\partial_p \varepsilon_{qs})}, \quad (3b)$$

where $\tau_{pq} = \tau_{qp}$ is the Cauchy (in Mindlin's notation) stress tensor and $m_{pqs} = m_{psq}$ is the dipolar (or double) stress tensor. The latter tensor follows from the notion of *multipolar* forces, which are antiparallel forces acting between the micro-media contained in the continuum with microstructure (see Fig. 1). As explained by Green and Rivlin [2] and Jaunzemis [26], the notion of multipolar forces arises rather naturally if one considers a series expansion for the mechanical power \mathcal{M} containing higher-order velocity gradients, i.e., $\mathcal{M} = F_p \dot{u}_p + F_{pq} (\partial_p \dot{u}_q) + F_{pqs} (\partial_p \partial_q \dot{u}_s) + \dots$, where F_p are the usual forces (monopolar forces) within classical continua and (F_{pq}, F_{pqs}, \dots) are the multipolar forces (dipolar or double forces, triple forces and so on) within generalized continua. In this way, the resultant force on an ensemble of subparticles can be viewed as being decomposed into *external* and *internal* forces with the latter ones being self-equilibrating (see Fig. 1). However, these self-equilibrating forces (which are multipolar forces) produce *nonvanishing* stresses, the multipolar stresses. Examples of force systems of the dipolar collinear or noncollinear type are given, e.g., in Jaunzemis [26] and Fung [27].

As for the notation of dipolar forces and stresses, the first index of the forces denotes the orientation of the lever arm between the forces and the second index the orientation of the pair of the forces; the same meaning is attached to the last two indices of the stresses, whereas the first index denotes the orientation of the normal to the surface on which the stress acts. The dipolar forces F_{pq} have dimensions of [force][length]; their diagonal terms are double forces without moment and their off-diagonal terms are double forces with moment. The antisymmetric part $F_{[pq]} = (1/2)(x_p F_q - x_q F_p)$ gives rise to couple stresses. Here, we do not consider couple-stress effects emphasizing that this is compatible with the particular choice of the form of W in (2), i.e., a form dependent upon the strain gradient but completely independent upon the rotation gradient.

Further, the equations of motion and the traction boundary conditions along a smooth boundary can be obtained either from Hamilton's principle (Mindlin [1]) or from the momentum balance laws and their application on a material tetrahedron (Georgiadis et al. [22]):

$$\partial_p (\tau_{pq} - \partial_s m_{spq}) = \rho \ddot{u}_q - \frac{\rho h^2}{3} (\partial_{pp} \ddot{u}_q), \quad (4)$$

$$n_q (\tau_{qs} - \partial_p m_{pqs}) - D_q (n_p m_{pqs}) + (D_l n_l) n_p n_q m_{pqs} + \frac{\rho h^2}{3} n_r (\partial_r \ddot{u}_s) = P_s^{(n)}, \quad (5a)$$

$$n_q n_r m_{qrs} = R_s^{(n)}, \quad (5b)$$

where body forces are absent, $D_p(\cdot) = \partial_p(\cdot) - n_p D(\cdot)$, $D(\cdot) = n_l \partial_l(\cdot)$, n_s is the unit outward-directed vector normal to the boundary, $P_s^{(n)}$ is the surface force per unit area (monopolar traction), and $R_s^{(n)}$ is the surface double force per unit area (dipolar traction).

Finally, it is convenient for calculations to introduce another quantity, which is a kind of "balance stress" (see Eq. (7) below), and is defined as

$$\sigma_{pq} = \tau_{pq} + \alpha_{pq}, \quad (6)$$

where $\alpha_{qs} = (\rho h^2/3)(\partial_q \ddot{u}_s) - \partial_p m_{pqs}$. With this definition, Eq. (4) takes the more familiar form

$$\partial_p \sigma_{pq} = \rho \ddot{u}_q. \quad (7)$$

Notice that σ_{pq} is not an objective quantity since it contains the acceleration terms $(\rho h^2/3)(\partial_q \ddot{u}_s)$. These micro-inertia terms also are responsible for the asymmetry of σ_{pq} . This, however, does not pose any inconsistency but reflects the role of micro-inertia and the nonstandard nature of the theory. In the quasi-static case, where the acceleration terms are absent, σ_{pq} is an objective tensor. On the other hand, the constitutive equations should definitely obey the principle of objectivity (cf. Eqs. (9) and (10) below).

Now, the simplest possible form of constitutive relations is obtained by taking an isotropic version of the expression in (2) involving only three material constants. This strain-energy density function reads

$$W = \frac{1}{2} \lambda \varepsilon_{pp} \varepsilon_{qq} + \mu \varepsilon_{pq} \varepsilon_{pq} + \frac{1}{2} \lambda c (\partial_s \varepsilon_{pp}) (\partial_s \varepsilon_{qq}) + \mu c (\partial_s \varepsilon_{pq}) (\partial_s \varepsilon_{pq}), \quad (8)$$

and leads to the constitutive relations

$$\tau_{pq} = \lambda \delta_{pq} \varepsilon_{ss} + 2\mu \varepsilon_{pq}, \quad (9)$$

$$m_{spq} = c \partial_s (\lambda \delta_{pq} \varepsilon_{jj} + 2\mu \varepsilon_{pq}), \quad (10)$$

where (λ, μ) are the standard Lamé's constants, c is the gradient coefficient (material constant with dimensions of [length]²), and δ_{pq} is the Kronecker delta. Equations (9) and (10) written for a general three-dimensional state will be employed below only for an antiplane shear state.

In summary, Eqs. (4), (5), (9), and (10) are the governing equations for the isotropic dipolar-gradient elasticity with no couple stresses. Combining (4), (9), and (10) leads to the field equation of the problem. Pertinent *uniqueness* theorems have been proved for various forms of the general theory (Mindlin and Eshel [4], Achenbach et al. [9], and Ignaczak [28]) on the basis of *positive definiteness* of the strain-energy density. The latter restriction requires, in turn, the following inequalities for the material constants appearing in the theory employed here (Georgiadis et al. [22]): $(3\lambda + 2\mu) > 0$, $\mu > 0$, $c > 0$. In addition, *stability* for the field equation in the general inertial case was proved in [22] and to accomplish this the condition $c > 0$ is a necessary one (we notice incidentally that some heuristic gradient-like approaches not employing the rigorous Mindlin-Green-Rivlin theory appeared in the literature that take a negative c —their authors, unfortunately, do not realize that stability was lost in their field equation). Finally, the analysis in [22] provides the order-of-magnitude estimate $(0.1h)^2$ for the gradient coefficient c , in terms of the intrinsic material length h .

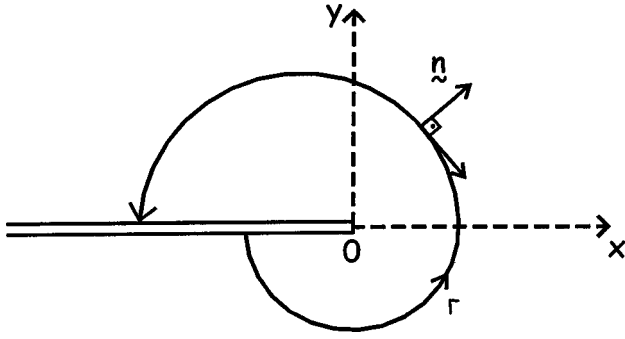


Fig. 2 A crack under a remotely applied antiplane shear loading. The contour Γ surrounding the crack tip serves for the definition of the J -integral.

3 Formulation of the Quasi-Static Mode III Crack Problem, the J -Integral, and the Energy Release Rate

Consider a crack in a body with microstructure under a quasi-static antiplane shear state (see Fig. 2). As will become clear in the next two sections, the semi-infinite crack model serves in a *boundary layer* type of analysis of any crack problem provided that the crack faces in the problem under consideration are traction free. It is assumed that the mechanical behavior of the body is determined by the Eqs. (4), (5), (9), and (10) of the previous section. An $Oxyz$ Cartesian coordinate system coincident with the system $Ox_1x_2x_3$ utilized previously is attached to that body, and an antiplane shear loading is taken in the direction of z -axis. Also, a *pure* antiplane shear state will be reached, if the body has the form of a thick slab in the z -direction. In such a case, the following two-dimensional field is generated:

$$u_x = u_y = 0, \quad (11a)$$

$$u_z \equiv w \neq 0, \quad (11b)$$

$$w \equiv w(x, y), \quad (11c)$$

and Eqs. (8)–(10) take the forms

$$W = \mu(\varepsilon_{xz}^2 + \varepsilon_{yz}^2) + \mu c \left[\left(\frac{\partial \varepsilon_{xz}}{\partial x} \right)^2 + \left(\frac{\partial \varepsilon_{xz}}{\partial y} \right)^2 + \left(\frac{\partial \varepsilon_{yz}}{\partial x} \right)^2 + \left(\frac{\partial \varepsilon_{yz}}{\partial y} \right)^2 \right], \quad (12)$$

$$\tau_{xz} = \mu \frac{\partial w}{\partial x}, \quad (13a)$$

$$\tau_{yz} = \mu \frac{\partial w}{\partial y}, \quad (13b)$$

$$m_{xxz} = \mu c \frac{\partial^2 w}{\partial x^2}, \quad (14a)$$

$$m_{xyz} = \mu c \frac{\partial^2 w}{\partial x \partial y}, \quad (14b)$$

$$m_{yxz} = \mu c \frac{\partial^2 w}{\partial x \partial y}, \quad (14c)$$

$$m_{yyz} = \mu c \frac{\partial^2 w}{\partial y^2}. \quad (14d)$$

Further, (4) provides the equation of equilibrium

$$\frac{\partial}{\partial x} \left(\tau_{xz} - \frac{\partial m_{xxz}}{\partial x} - \frac{\partial m_{yxz}}{\partial y} \right) + \frac{\partial}{\partial y} \left(\tau_{yz} - \frac{\partial m_{xyz}}{\partial x} - \frac{\partial m_{yyz}}{\partial y} \right) = 0, \quad (15)$$

which along with (13) and (14) leads to the following field equation of the problem

$$c \nabla^4 w - \nabla^2 w = 0, \quad (16)$$

where $\nabla^2 = (\partial^2/\partial x^2) + (\partial^2/\partial y^2)$ and $\nabla^4 = \nabla^2 \nabla^2$. Finally, one may utilize σ_{pq} defined in (6) for more economy in writing some equations in the ensuing analysis. The antiplane shear components of this quantity are as follows:

$$\sigma_{xz} = \mu \left(\frac{\partial w}{\partial x} \right) - \mu c \nabla^2 \left(\frac{\partial w}{\partial x} \right), \quad (17a)$$

$$\sigma_{yz} = \mu \left(\frac{\partial w}{\partial y} \right) - \mu c \nabla^2 \left(\frac{\partial w}{\partial y} \right). \quad (17b)$$

Assume now that the cracked body is under a *remotely* applied loading that is also *antisymmetric* about the x -axis (crack plane). Also, the crack faces are traction-free. Due to the antisymmetry of the problem, only the upper half of the cracked domain is considered. Then, the following conditions can be written along the plane ($-\infty < x < \infty, y = 0$):

$$t_{yz} \equiv \tau_{yz} - \frac{\partial m_{xyz}}{\partial x} - \frac{\partial m_{yyz}}{\partial y} - \frac{\partial m_{yxz}}{\partial x} = 0 \quad \text{for } (-\infty < x < 0, y = 0), \quad (18)$$

$$m_{yyz} = 0 \quad \text{for } (-\infty < x < 0, y = 0), \quad (19)$$

$$w = 0 \quad \text{for } (0 < x < \infty, y = 0), \quad (20)$$

$$\frac{\partial^2 w}{\partial y^2} = 0 \quad \text{for } (0 < x < \infty, y = 0), \quad (21)$$

where (18) and (19) directly follow from Eqs. (5) (notice also that (18) can be written as $\sigma_{yz} - (\partial m_{yxz}/\partial x) = 0$ by using the σ_{pq} quantity), t_{yz} is defined as the *total monopolar stress*, and (20) together with (21) always guarantee an antisymmetric displacement field w.r.t. the line of the crack prolongation. The definition of the stress t_{yz} follows from (5a). The problem described by (11)–(21) will be considered by both the asymptotic Williams method and the exact Wiener-Hopf technique. Notice finally that no difficulty will arise by having zero boundary conditions along the crack faces since, eventually, the solution will be matched at regions where gradient effects are not dominant (i.e., for $x \gg c^{1/2}$) with the K_{III} field of the classical theory and in this way the remote loading will appear in the solution.

Next, we present the new extended definitions of the J -integral and the energy release rate G . These definitions of the energy quantities are pertinent to the present framework of dipolar gradient elasticity and to the aforementioned case of a crack in a quasi-static antiplane shear state. By following relative concepts from Rice [29,30], we first introduce the definition

$$J = \int_{\Gamma} \left(W dy - \bar{P}_z^{(n)} \frac{\partial w}{\partial x} d\Gamma - \bar{R}_z^{(n)} D \left(\frac{\partial w}{\partial x} \right) d\Gamma \right), \quad (22)$$

where Γ is a two-dimensional contour surrounding the crack tip (see Fig. 2), whereas the monopolar and dipolar tractions $\bar{P}_z^{(n)}$ and $\bar{R}_z^{(n)}$ on Γ are given as

$$\bar{P}_z^{(n)} = n_q (\tau_{qz} - \partial_p m_{pqz}) - D_q (n_p m_{pqz}) + (D_l n_l) n_p n_q m_{pqz}, \quad (23a)$$

$$\bar{R}_z^{(n)} = n_p n_q m_{pqz}. \quad (23b)$$

In the above expressions, n_p with components (n_x, n_y) is the unit outward-directed vector normal to Γ , the differential operators D and D_p were defined in Section 2, W is the strain-energy density function given by (12), and the indices (l, p, q) take the values x and y only.

Of course, the above expressions for the tractions on Γ are compatible with Eqs. (5). Further, it can be proved that the integral in (22) is path independent by following Rice's, [29], procedure. Path independence is of great utility since it permits alternate choices of integration paths that may lead to a direct

evaluation of J . We should mention at this point that (22) is quite novel within the present version of the gradient theory (i.e., a form *without* couple stresses), but expressions for J within the couple-stress theory were presented before by Atkinson and Leppington [31], Zhang et al. [18], and Lubarda and Markenscoff [32]. In particular, the latter work gives a systematic derivation of conservation integrals by the use of Noether's theorem. Finally, we no-

tice that the way the J -integral will be evaluated below is quite different than that by Zhang et al. [18]. Indeed, use of the theory of distributions in the present work leads to a very simple way to evaluate J (see Section 7 below).

As for the energy release rate (ERR) now, we also modify the classical definition in order to take into account a higher-order term that is compatible with the present strain-gradient framework

$$G = \lim_{\Delta x \rightarrow 0} \frac{\int_0^{\Delta x} \left[t_{yz}(x, y=0) \cdot w(x, y=0) + m_{yyz}(x, y=0) \cdot \frac{\partial w(x, y=0)}{\partial y} \right] dx}{\Delta x}, \quad (24)$$

where Δx is the small distance of a crack advancement.

Of course, any meaningful crack-tip field given as solution to an associated mathematical problem, should result in a *finite* value for the energy quantities defined above. Despite the strong singularity of the stress field obtained in Sections 5 and 6, the results of Section 7 prove that J and G are indeed bounded.

4 Asymptotic Analysis by the Williams Method

As is well known, Williams [33,34] (see also Barber [35]) developed a method to explore the nature of the stress and displacement field near wedge corners and crack tips. This is accomplished by attaching a set of (r, θ) polar coordinates at the corner point and by expanding the stress field as an asymptotic series in powers of r . By following this method here we are concerned, in a way, only with the field components in the sharp crack at very small values of r , and hence we imagine looking at the tip region through a strong microscope so that situations like the ones, e.g., on the left of Fig. 3 (i.e., a finite length crack, an edge crack or a crack in a strip) appear to us like the semi-infinite crack on the right of this figure. The magnification is so large that the other surfaces of the body, including the loaded remote boundaries, appear enough far away for us to treat the body as an "infinite wedge" with "loading at infinity." The field is, of course, a complicated function of (r, θ) but near to the crack tip (i.e., as $r \rightarrow 0$) we seek to expand it as a series of separated variable terms, each of which satisfies the traction-free boundary conditions on the crack faces.

In view of the above, we consider the following separated form $w(r, \theta) = r^{\omega+1} u(\theta)$, where the displacement satisfies (16). Further, if only the dominant singular terms in (16) are retained, the PDE of the problem becomes $\nabla^4 w = 0$, where $\nabla^4 = \nabla^2 \nabla^2 = (\partial^2/\partial r^2 + 1/r \partial/\partial r + 1/r^2 \partial^2/\partial \theta^2)^2$. Also, in view of the definitions of stresses as combinations of derivatives of w and by re-

taining again only the dominant singular terms, the boundary conditions $t_{yz}(x, y = \pm 0) = 0$ and $m_{yyz}(x, y = \pm 0) = 0$ will give at $\theta = \pm \pi$

$$\left(\frac{\partial^2}{\partial r^2} + \frac{1}{r^2} \frac{\partial^2}{\partial \theta^2} + \frac{1}{r^2} \right) \frac{\partial w}{\partial \theta} = 0, \quad (25a)$$

$$\left(\frac{1}{r} \frac{\partial}{\partial r} + \frac{1}{r^2} \frac{\partial^2}{\partial \theta^2} \right) w = 0. \quad (25b)$$

In addition, the pertinent antisymmetric solution (i.e., with odd behavior in θ) to the equation $\nabla^4 w = 0$ has the following general form:

$$w = r^{\omega+1} (A_1 \sin[(\omega+1)\theta] + A_2 \sin[(\omega-1)\theta]), \quad (26)$$

where ω is (in general) a complex number and (A_1, A_2) are unknown constants. Now, (25) and (26) provide the *eigenvalue* problem

$$(\omega+1) \cos[(\omega+1)\pi] \cdot A_1 - 3(\omega-1) \cos[(\omega-1)\pi] \cdot A_2 = 0, \quad (27a)$$

$$(\omega+1) \sin[(\omega+1)\pi] \cdot A_1 + (\omega-3) \sin[(\omega-1)\pi] \cdot A_2 = 0. \quad (27b)$$

For a nontrivial solution to exist, the determinant of the coefficients of (A_1, A_2) in the above system should vanish and this gives the result: $\sin(2\omega\pi) = 0 \Rightarrow \omega = 0, 1/2, 1, 3/2, 2, \dots$. Next, by observing from (12) that the strain-energy density W behaves at most as $(\partial^2 w / \partial r^2)$ or, by using the form $w(r, \theta) = r^{\omega+1} u(\theta)$, no worse than $r^{\omega-1}$, we conclude that the maximum eigenvalue allowed by the *integrability* condition of the strain-energy density is $\omega = 1/2$.

The above analysis suggests that the general asymptotic solution is of the form $w(r, \theta) = r^{3/2} u(\theta)$, which by virtue of (26) and (27b) becomes

$$w(r, \theta) = A r^{3/2} [3 \sin(\theta/2) - 5 \sin(3\theta/2)], \quad (28)$$

where $A \equiv -A_1$ and the other constant in (26) is given by (27b) as $A_2 = 3A_1/5$. The constant A (amplitude of the field) is left unspecified by the Williams technique but still the nature of the near-tip field has been determined. Finally, the total monopolar stress has the following asymptotic behavior:

$$t_{yz}(x, y=0) = O(x^{-3/2}) \quad \text{as } x \rightarrow +0. \quad (29)$$

This asymptotic behavior will also be corroborated by the results of the exact analysis in the next section.

5 Exact Analysis by the Wiener-Hopf Method

An *exact* solution to the problem described by (11)–(21) will be obtained through two-sided Laplace transforms (see, e.g., van der Pol and Bremmer [36] and Carrier et al. [37]), the Wiener-

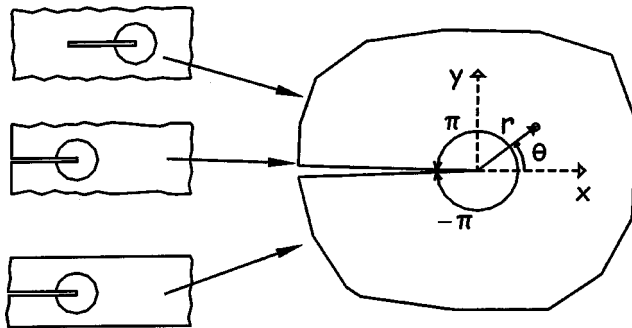


Fig. 3 Williams' method: the near-tip fields of (i) a finite length crack, (ii) an edge crack, and (iii) a cracked strip correspond to the field generated in a body with a semi-infinite crack

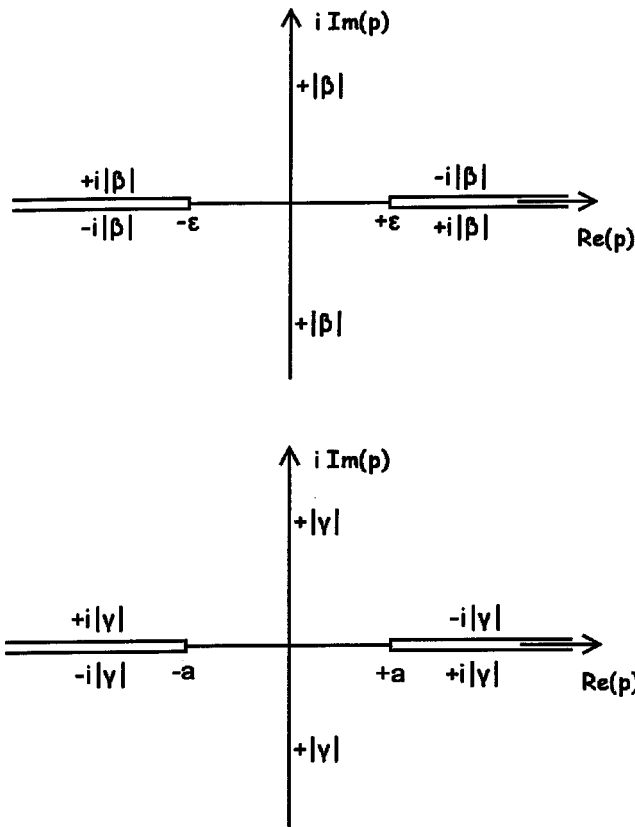


Fig. 4 Branch cuts for the functions (β, γ)

Hopf technique (see, e.g., Roos [38] and Mittra and Lee [39]) and certain results from the theory of distributions (see, e.g., Gel'fand and Shilov [40] and Lauwerier [41]).

The direct and inverse two-sided Laplace transforms are defined as

$$f^*(p, y) = \int_{-\infty}^{\infty} f(x, y) e^{-px} dx, \quad (30a)$$

$$f(x, y) = \frac{1}{2\pi i} \int_{Br} f^*(p, y) e^{px} dp, \quad (30b)$$

where Br denotes the Bromwich inversion path *within* the region of analyticity of the function $f^*(p, y)$ in the complex p -plane. Transforming (16) with (30a) gives the ODE

$$c \frac{d^4 w^*}{dy^4} + (2cp^2 - 1) \frac{d^2 w^*}{dy^2} + (cp^4 - p^2) w^* = 0. \quad (31)$$

The above equation has the following general solution that is bounded as $y \rightarrow +\infty$

$$w^*(p, y) = B(p) \cdot \exp(-\beta y) + C(p) \cdot \exp(-\gamma y) \quad \text{for } y \geq 0, \quad (32)$$

where $B(p)$ and $C(p)$ are yet unknown functions, $\beta \equiv \beta(p) = (\varepsilon^2 - p^2)^{1/2}$ with ε being a real number such that $\varepsilon \rightarrow +0$, and $\gamma \equiv \gamma(p) = [(1/c) - p^2]^{1/2} \equiv (a^2 - p^2)^{1/2}$ with $a = (1/c)^{1/2}$. In fact, introducing ε facilitates the introduction of the branch cuts for $\beta = (-p^2)^{1/2}$ -cf. [20] and [37] for this procedure as applied to related situations. To obtain a bounded solution as $y \rightarrow +\infty$, the p -plane should be cut in the way shown in Fig. 4. This introduction of branch cuts secures that the functions (β, γ) are single-valued and that $\text{Re}(\beta) > 0$ and $\text{Re}(\gamma) > 0$ along the Bromwich path.

The transformed expressions for the stresses that enter the boundary conditions are also quoted (for convenience, the σ_{yz} quantity is employed in the boundary conditions)

$$\sigma_{yz}^*(p, y) = -\mu B \beta e^{-\beta y}, \quad (33)$$

$$m_{yz}^*(p, y) = \mu (Bc \beta^2 e^{-\beta y} + Cc \gamma^2 e^{-\gamma y}), \quad (34)$$

$$m_{yxz}^*(p, y) = -\mu p (Bc \beta e^{-\beta y} + Cc \gamma e^{-\gamma y}). \quad (35)$$

Next, in preparation for formulating the Wiener-Hopf equation, the one-sided Laplace transforms of the unknown total monopolar stress $t_{yz}(x > 0, y = 0)$ ahead of the crack tip and the unknown crack-face displacement $w(x < 0, y = 0)$ are defined

$$T^+(p) = \int_0^{\infty} t_{yz}(x, y = 0) e^{-px} dx \equiv \int_0^{\infty} \left[\sigma_{yz}(x, y = 0) - \frac{\partial m_{yxz}(x, y = 0)}{\partial x} \right] e^{-px} dx, \quad (36)$$

$$W^-(p) = \int_{-\infty}^0 w(x, y = 0) e^{-px} dx. \quad (37)$$

Further, we assume the following *finiteness* conditions at $x \rightarrow \pm\infty$: $|t_{yz}(x, y = 0)| < M \cdot \exp(-p_T x)$ for $x \rightarrow +\infty$ and $|w(x, y = 0)| < N \cdot \exp(p_W x)$ for $x \rightarrow -\infty$, where (M, N, p_T, p_W) are positive constants. As a consequence, $T^+(p)$ is analytic and defined in the right half-plane $-p_T < \text{Re}(p)$ (the "plus" half-plane), while $W^-(p)$ is analytic and defined in the left half-plane $\text{Re}(p) < p_W$ (the "minus" half-plane).

Then, enforcement of boundary conditions results in the following equations:

$$T^+(p) = \sigma_{yz}^*(p, y = 0) - p \cdot m_{yxz}^*(p, y = 0), \quad (38)$$

$$W^-(p) = w^*(p, y = 0). \quad (39)$$

The above equations along with the equation $\partial^2 w^*(p, y = 0) / \partial y^2 = 0$, Eqs. (33)–(35) and the general solution in (32) provide an algebraic system of three equations in four unknowns (the functions T^+ , W^- , B , C). Finally, eliminating B and C in this system leads to the following Wiener-Hopf problem

$$\frac{T^+(p)}{(a+p)^{1/2}} = -\mu c p^2 (a-p)^{1/2} \cdot L(p) \cdot W^-(p), \quad (40)$$

where the kernel function $L(p)$ is given as

$$L(p) = -c p^2 \left[1 + \frac{1 - c p^2 (a^2 - p^2)^{1/2}}{c p^2 (\varepsilon^2 - p^2)^{1/2}} \right]. \quad (41)$$

The next target will be to determine both T^+ and W^- from the single Eq. (40). This will be effected through the use of elements of the theories of complex variables, integral transforms, and distributions (theorem of analytic continuation, extended Liouville's theorem, Abel-Tauber asymptotic theorems, transforms of distributions). First, we check that the function $L(p)$ has no zeros in the complex plane. This was found independently by using both the principle of the argument, [37], and the program MATHEMATICA™. We notice that unlike the current static case, the counterpart kernel function in the dynamic case exhibits two (nonextraneous) zeros, a fact that modifies somehow the standard Wiener-Hopf method. Further, we find that the asymptotic behavior of the kernel is $\lim_{|p| \rightarrow \infty} L(p) = -3/2$ and this leads us to introduce a modified kernel given as $N(p) = -(2/3) \cdot L(p)$, which possesses the desired asymptotic property $\lim_{|p| \rightarrow \infty} N(p) = 1$. Indeed, this new form of the kernel facilitates its *product splitting* by the use of Cauchy's integral theorem. The Wiener-Hopf equation takes now the form

$$\frac{T^+(p)}{(a+p)^{1/2}} = \left(-\frac{3}{2} \right) (-\mu c) p^2 (a-p)^{1/2} N(p) \cdot W^-(p), \quad (42)$$

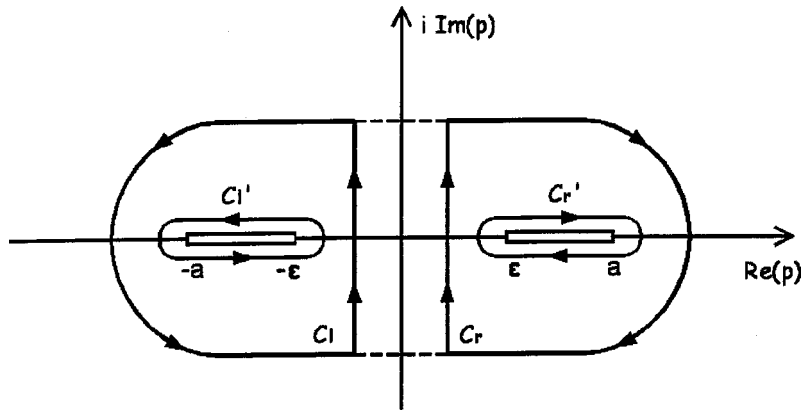


Fig. 5 Contour integrations for the factorization of the kernel function in Eq. (42)

and the kernel is written as the following product of two analytic and nonzero functions defined in pertinent half-plane domains of the complex plane, [38,39],

$$N(p) = N^+(p) \cdot N^-(p), \quad (43)$$

where

$$N^+(p) = \exp\left\{-\frac{1}{2\pi i} \int_{C_l} \frac{\ln[N(\zeta)]}{\zeta - p} d\zeta\right\}, \quad (44a)$$

$$N^-(p) = \exp\left\{\frac{1}{2\pi i} \int_{C_r} \frac{\ln[N(\zeta)]}{\zeta - p} d\zeta\right\}. \quad (44b)$$

The use of Cauchy's integral theorem is depicted in Fig. 5. $N^+(p)$ is analytic and nonzero in $\text{Re}(p) > -\varepsilon$ and $N^-(p)$ is analytic and nonzero in $\text{Re}(p) < \varepsilon$. The original integration paths (C_l, C_r) extend parallel to the imaginary axis in the complex ζ -plane. Finally, an alteration of the integration contour (also depicted in Fig. 5) along with use of Cauchy's theorem and Jordan's lemma allows taking as equivalent integration paths the (C_l', C_r') contours around the branch cuts extending along $-a < \zeta < -\varepsilon$ and $\varepsilon < \zeta < a$. This eventually leads to the following forms of the sectionally analytic functions $N^\pm(p)$:

$$N^\pm(p) = \exp\left\{\frac{1}{\pi} \int_0^a \arctan\left[\frac{(a^2 - \zeta^2)^{3/2}}{\zeta^3}\right] \frac{d\zeta}{\zeta \pm p}\right\}, \quad (45)$$

with the property $N^+(-p) = N^-(p)$.

With the product factorisation in hand, Eq. (42) takes the following form that defines a function $E(p)$:

$$\frac{T^+(p)}{N^+(p) \cdot (a+p)^{1/2}} = \frac{3\mu c}{2} p^2 (a-p)^{1/2} N^-(p) \cdot W^-(p) \equiv E(p). \quad (46)$$

The above equation defines $E(p)$ only in the strip $-\varepsilon < \text{Re}(p) < 0$. But the first member in the equation is a nonzero analytic function in $\text{Re}(p) > -\varepsilon$, and the second member is a nonzero analytic function in $\text{Re}(p) < 0$. Then, in view of the theorem of analytic continuation (or identity theorem for single-valued analytic functions), the two members define one and the same function that is analytic over the whole p -plane, [38,39]. In other words, $E(p)$ is an entire function. Polynomial and exponential functions are the types of entire functions. The case of an exponential function (i.e., a function of the form $\exp[g(p)]$, where $g(p)$ is a polynomial) should be excluded because such a function has an essential singularity at infinity. Indeed, an exponential growth of the functions involved in (46) would result in violating the so-called edge condition, i.e., the condition of bounded energy density around the geometrical singularity (crack edge) in the physical domain.

Therefore, $E(p)$ should be a polynomial since only algebraic growth of the fields in the neighborhood of the crack tip is allowed. Further, determining the coefficients of this polynomial will lead to the desired decoupling of $T^+(p)$ and $W^-(p)$. Below, we determine the form of $E(p)$ by the use of asymptotic analysis.

In particular, we will use theorems of the Abel and Tauber type having the form

$$\lim_{x \rightarrow 0} f(x) \overset{\text{LT}}{\leftrightarrow} \lim_{|p| \rightarrow \infty} f^*(p), \quad (47)$$

$$\lim_{x \rightarrow \infty} f(x) \overset{\text{LT}}{\leftrightarrow} \lim_{|p| \rightarrow 0} f^*(p), \quad (48)$$

where the symbol $\overset{\text{LT}}{\leftrightarrow}$ means that the image function $f^*(p)$ and the original function $f(x)$ are connected through the one-sided Laplace-transform relations $f^*(p) = \int_0^\infty f(x) e^{-px} dx$ and $f(x) = (1/2\pi i) \int_B f^*(p) e^{px} dp$, and p is a complex variable which in (47) and (48) tends to infinity or zero along paths in the pertinent half-plane of convergence (analyticity). Relations (47) and (48) hold under certain conditions given, e.g., in [36]. Also, the extended Liouville's theorem, [39], will be utilized. Referring to (46), this states that if $T^+(p) \cdot [N^+(p) \cdot (a+p)^{1/2}]^{-1} = O(p^\nu)$ and $(3\mu c/2) p^2 (a-p)^{1/2} N^-(p) \cdot W^-(p) = O(p^\xi)$ in the respective half-planes of analyticity, then $E(p)$ is a polynomial of degree not exceeding the minimum of $([\nu], [\xi])$, where the symbol $[]$ denotes the integral part of a number.

Now as a first possibility of the near-tip behavior, one may adopt a behavior of the total monopolar stress and the crack-face displacement that is analogous to the classical fracture mechanics behavior, viz.

$$t_{yz}(x, y=0) = O(x^{-1/2}) \quad \text{as } x \rightarrow +0, \quad (49a)$$

$$w(x, y=0) = O(x^{1/2}) \quad \text{as } x \rightarrow -0. \quad (49b)$$

This field gives by (47) and the transformation formula $x^\kappa \overset{\text{LT}}{\leftrightarrow} \Gamma(\kappa+1) \cdot p^{-\kappa-1}$ (with $\Gamma(\cdot)$ being the Gamma function and $\kappa > -1$), [36,38], the following asymptotic behavior in the transform domain

$$T^+(p) = O(p^{-1/2}) \quad \text{as } |p| \rightarrow \infty, \quad (50a)$$

$$W^-(p) = O(p^{-3/2}) \quad \text{as } |p| \rightarrow \infty. \quad (50b)$$

Then, Liouville's theorem leads to the conclusion that $E(p) = 0$, which, however, is an inadmissible result since it shows that the stress field is zero everywhere (although the cracked body is under loading). Therefore, the possibility of a near-tip behavior given by (49) should be discarded.

Next, prompted by the results of the Williams asymptotic method obtained before, i.e., the results in (28) and (29), we consider the following possibility of near-tip behavior

$$t_{yz}(x,y=0) = O(x^{-3/2}) \quad \text{as } x \rightarrow +0, \quad (51a)$$

$$w(x,y=0) = O(x^{3/2}) \quad \text{as } x \rightarrow -0. \quad (51b)$$

Here, certain results of the theory of generalized functions will be employed concerning transforms of *singular* distributions, [40,41]. In this connection, we note that the distribution x_+^λ for $\text{Re}(\lambda) > -1$ is identified with the function $x_+^\lambda = x^\lambda$ for $x > 0$ and $x_+^\lambda = 0$ for $x < 0$. For other values of the complex parameter λ (of course, λ here is not to be confused with the Lamé constant) it is defined by analytic continuation of the functional $\langle x_+^\lambda, h \rangle \equiv \int_0^\infty x^\lambda h(x) dx$, where $h(x)$ is a test function. In this way, a distribution is obtained for all complex values of λ with the exception of $\lambda = -1, -2, -3, \dots$. In a similar manner, x_-^λ is defined by starting from $x_-^\lambda = 0$ for $x > 0$ and $x_-^\lambda = |x|^\lambda$ for $x < 0$. Then, (51) and the transformation formula $x^\lambda \xleftrightarrow{\text{LT}} \Gamma(\lambda + 1) \cdot p^{-\lambda-1}$ (with $\lambda \neq -1, -2, -3, \dots$), [40,41], provide the following asymptotic behavior in the transform domain:

$$T^+(p) = O(p^{1/2}) \quad \text{as } |p| \rightarrow \infty, \quad (52a)$$

$$W^-(p) = O(p^{-5/2}) \quad \text{as } |p| \rightarrow \infty. \quad (52b)$$

Further the extended Liouville's theorem leads to the conclusion that $E(p) = E_0$, where E_0 is a constant. As shown below this constant will be determined from conditions at remote regions in the physical plane. The previous result is mathematically admissible, while any other case like, e.g., $t_{yz}(x,y=0) = O(x^{-1})$ or $O(x^{-2})$ as $x \rightarrow +0$ is precluded since even analytic continuation fails to define one-sided Laplace (or Fourier) transforms of the associated singular distributions (cf. Gel'fand and Shilov [40], p. 171). Of course, it remains to prove that the field in (51) gives a *bounded* value for the energy quantities of *J*-integral and ERR, despite the hypersingular character of stress. This will be shown in Section 7. Finally, the requirement of boundedness of energy expressions is not only to be imposed on physical grounds but it is generally (Ignaczak [28] and Knowles and Pucik [42]) a necessary condition for uniqueness.

Our task now is to determine E_0 . As in the work of Zhang et al. [18], a matching procedure is followed that equates the *inner* solution $\lim_{x \rightarrow \infty} t_{yz}(x,y=0)$, as obtained by the present gradient analysis, with the *outer* solution $K_{\text{III}}/(2\pi x)^{1/2}$ provided by the conventional fracture mechanics. K_{III} is the stress intensity factor for each specific problem treated by the conventional fracture mechanics. The latter field (singular solution) dominates over an area that is relatively close to the crack tip but lies outside the domain where gradient effects are pronounced. We notice the following in support of the assertion that this procedure is indeed reasonable: (i) as shown below the stress behaves as $t_{yz} = O(x^{-1/2})$ for $x \rightarrow \infty$, (ii) the very form of the field Eq. (16) exhibits the singular-perturbation character of the gradient formulation and therefore suggests a *boundary layer* approach (Van Dyke [43]) to the crack problem (one may observe that an extremely small quantity—the coefficient c —multiplies the higher-order term, which is the one introduced by the nonconventional formulation). Finally, one may observe that this concept is in some respects similar to the one introduced by Rice [44] in analyzing small scale yielding around a crack tip.

The transformed total monopolar stress $T^+(p)$ is given by (46) as

$$T^+(p) = E_0 \cdot N^+(p) \cdot (a+p)^{1/2}, \quad (53)$$

an expression that holds for *all* values of the Laplace transform variable p in the right half-plane. For the moment, we need to evaluate only $\lim_{|p| \rightarrow 0} T^+(p)$ in order to obtain then $\lim_{x \rightarrow \infty} t_{yz}(x,y=0)$ by (48). One way to obtain the expression of

$\lim_{|p| \rightarrow 0} N^+(p)$ is to use $\lim_{|p| \rightarrow 0} N(p)$ and perform a product factorization of the latter limit by *inspection*. This way is easier than finding $\lim_{|p| \rightarrow 0} N^+(p)$ from (45). Indeed, one may obtain first from (41) and the definition of $N(p)$ the limit $\lim_{|p| \rightarrow 0} N(p) = 2(3c^{1/2})^{-1}(\varepsilon^2 - p^2)^{-1/2}$ and then

$$\lim_{|p| \rightarrow 0} N^+(p) = \left(\frac{2}{3c^{1/2}} \right)^{1/2} \frac{1}{(\varepsilon + p)^{1/2}}. \quad (54)$$

Further, a combination of (53) and (54) provides the limit

$$\lim_{|p| \rightarrow 0} T^+(p) = E_0 \cdot \left(\frac{2}{3c} \right)^{1/2} \frac{1}{p^{1/2}}, \quad (55)$$

which by (48) and the transformation formula $x^\kappa \xleftrightarrow{\text{LT}} \Gamma(\kappa + 1) \cdot p^{-\kappa-1}$ (with $\kappa > -1$) allows writing

$$\lim_{x \rightarrow +\infty} t_{yz}(x,y=0) = E_0 \cdot \left(\frac{2}{3c} \right)^{1/2} \frac{1}{(\pi x)^{1/2}}. \quad (56)$$

Finally, matching the above expression with $K_{\text{III}}/(2\pi x)^{1/2}$ provides the value of the constant as $E_0 = K_{\text{III}}(3c)^{1/2}/2$.

In view of the above, we record the final transformed expressions (valid for all p in the pertinent half-plane of convergence) for the total monopolar stress ahead of the tip and the crack-face displacement

$$T^+(p) = \frac{K_{\text{III}}(3c)^{1/2}}{2} N^+(p) \cdot (a+p)^{1/2}, \quad (57)$$

$$W^-(p) = \frac{K_{\text{III}}}{(3c)^{1/2} \mu p^2 (a-p)^{1/2} \cdot N^-(p)}, \quad (58)$$

where it is reminded that $a = (1/c)^{1/2}$, and $N^+(p)$ and $N^-(p)$ are given by (45). Exact expressions for the original functions $t_{yz}(x > 0, y = 0)$ and $w(x < 0, y = 0)$ can be derived from (57) and (58) through one-sided Laplace-transform inversions. Such an inversion will be performed in Section 8, where we elaborate more on the stress ahead of the crack tip providing the exact expression and several comparisons. In closing now this section, we give the near-tip asymptotic expressions of $t_{yz}(x > 0, y = 0)$ and $w(x < 0, y = 0)$. These expressions, however, suffice for the evaluation of the *J*-integral and the ERR and possess also much practical importance as explained below.

The limits of the expressions in (57) and (58) for $|p| \rightarrow \infty$ are found to be

$$\lim_{|p| \rightarrow \infty} T^+(p) = \frac{K_{\text{III}}(3c)^{1/2}}{2} p^{1/2}, \quad (59)$$

$$\lim_{|p| \rightarrow \infty} W^-(p) = \frac{K_{\text{III}}}{(3c)^{1/2} \mu} p^{5/2}, \quad (60)$$

which by the inversions $p^{1/2} \xleftrightarrow{\text{LT}} [\Gamma(-1/2)]^{-1} x^{-3/2} = -(2\pi^{1/2})^{-1} x^{-3/2}$ and $p^{5/2} \xleftrightarrow{\text{LT}} [\Gamma(5/2)]^{-1} (-x)^{3/2} = 4(3\pi^{1/2})^{-1} (-x)^{3/2}$ give the following near-tip field

$$\lim_{x \rightarrow +0} t_{yz}(x,y=0) = -\frac{K_{\text{III}}(3c)^{1/2}}{4\pi^{1/2}} \frac{1}{x^{3/2}}, \quad (61)$$

$$\lim_{x \rightarrow -0} w(x,y=0) = \frac{4K_{\text{III}}}{3(3\pi c)^{1/2} \mu} (-x)^{3/2}. \quad (62)$$

In view of the fact that K_{III} is the stress intensity factor obtained by a classical elasticity analysis for the same crack problem (same geometry and loading) as that considered through the dipolar gradient approach, Eqs. (61) and (62) provide a kind of *correspondence principle*. This correspondence principle connects any classical fracture mechanics solution (through the pertinent K_{III} value

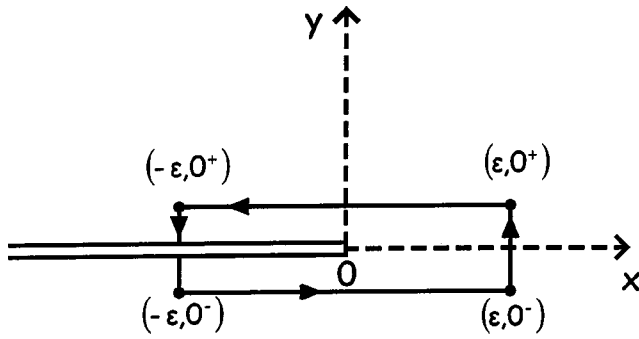


Fig. 6 Rectangular-shaped contour surrounding the crack tip for the evaluations of the J -integral and the energy release rate

obtained for each specific problem) with the near-tip field resulting by the nonclassical gradient formulation of the problem in question. Thus, a host of classical fracture mechanics solutions to crack problems may serve within a nonclassical gradient framework as well.

Three final notices pertain to the form of the above asymptotic field. First, the cusp-like closure of the crack faces (a closure smoother than the one predicted by the classical theory) implied by (62) is not unusual in experiments (see, e.g., Mills [45] and Ellsner et al. [46]). Secondly, an aggravation of the stress field as compared to the respective result of the conventional theory (this aggravation appears here through the stronger $x^{-3/2}$ singularity) is not unusual in analyses with nonclassical effects (see, e.g., the couple-stress results of Boggy and Sternberg [47] and Zhang et al. [18]). In addition, Prakash et al. [48] have provided an analysis and experimental evidence supporting the possibility of an $x^{-3/2}$ stress singularity in dynamic crack initiation. All this evidence shows that deviations from predictions of classical fracture mechanics are possible in some situations and are, at least, worthy of investigation. Of course, by no means we claim that the results in (61) and (62) carry over to other situations like, e.g., the plane strain/stress case. An appropriate dipolar gradient analysis for the latter case is needed to give the answer. Thirdly, the minus sign in the RHS of (61) shows that the asymptotic gradient crack-tip stress field has a cohesive-traction nature. This point will be further elaborated in Section 8 below. It will be shown also in Section 8 that (61) dominates only within an extremely small region adjacent to the crack tip.

6 Evaluation of the J -Integral and the Energy Release Rate (ERR)

The evaluation of the energy quantities is accomplished here by using Fisher's theorem, [49], concerning the product of distributions. For the J -integral, we also consider the new rectangular-shaped contour Γ (see Fig. 6) with vanishing "height" along the y -direction and with $\varepsilon \rightarrow +0$. This change of contour permits using solely the asymptotic near-tip field in (61) and (62). Notice that Zhang et al. [18] in evaluating the ERR for a mode III crack problem with couple stresses followed a rather involved method based on earlier work by Bueckner [50]. It seems that the procedure followed here is simpler and more direct. Indeed, taking into account (14d), (18), (19), and (21), the definitions in (22) and (24) provide the following integral for both energy quantities:

$$J = G = \lim_{\varepsilon \rightarrow +0} \left\{ 2 \int_{-\varepsilon}^{\varepsilon} t_{yz}(x, y=0) \cdot \frac{\partial w(x, y=0)}{\partial x} dx \right\}. \quad (63)$$

Now, by using the solution (61) and (62), we obtain

$$J = G = \lim_{\varepsilon \rightarrow +0} \left\{ 2(-1) \frac{K_{III}(3c)^{1/2}}{4\pi^{1/2}} \times \frac{4K_{III}}{3(3\pi c)^{1/2}\mu} \frac{3}{2} \int_{-\varepsilon}^{\varepsilon} (x_+)^{-3/2} (x_-)^{1/2} dx \right\}. \quad (64)$$

Further, the product of distributions inside the integral is obtained through the use of Fisher's theorem, [49], i.e., of the operational relation $(x_-)^\lambda (x_+)^{-1-\lambda} = -\pi \delta(x) [2 \sin(\pi\lambda)]^{-1}$ with $\lambda \neq -1, -2, -3, \dots$ and $\delta(x)$ being the Dirac delta distribution. Then, in view of the fundamental property of the Dirac delta distribution that $\int_{-\varepsilon}^{\varepsilon} \delta(x) dx = 1$, Eq. (64) provides the result

$$J = G = \frac{K_{III}^2}{2\mu}, \quad (65)$$

which shows that the J -integral and the ERR are *bounded* (despite the hypersingular nature of the near-tip stress) and identical with the respective classical elasticity result. Our findings suggest therefore that, at least for the one-parameter theory of microstructure employed here, the *overall* energy situation (rate of total potential energy) of the cracked body is not affected by the material microstructure and only the *local* crack-tip field is influenced.

7 Exact Expression for the Stress Ahead of the Crack Tip

In this section we elaborate more on the stress ahead of the crack tip $t_{yz}(x > 0, y = 0)$ and its nature, and also provide comparisons of the exact expression with both the asymptotic form in (61) and the classical $x^{-1/2}$ field. First, an exact one-sided Laplace transform inversion of $T^+(p)$ in (57) will be obtained.

One may write formally

$$t_{yz}(x > 0, y = 0) = \frac{K_{III}(3c)^{1/2}}{2} \frac{1}{2\pi i} \int_{Br} [N^+(p) \cdot (a+p)^{1/2}] e^{px} dp \equiv \frac{K_{III}(3c)^{1/2}}{2} \frac{1}{2\pi i} I, \quad (66)$$

where the integration variable takes values only in the half-plane $\text{Re}(p) > -\varepsilon$ ($\varepsilon \rightarrow +0$) and any line, in this half-plane, parallel to the $\text{Im}(p)$ -axis may serve as the Bromwich path. The I -integral defined above depends upon x and c . I is evaluated by deforming the integration path in the left half-plane (see Fig. 7) where the integrand is nonanalytic, exploiting in this way the existence of branch cuts for the functions $N^+(p)$ and $(a+p)^{1/2}$. Noting the property $\lim_{|p| \rightarrow \infty} N^+(p) = 1$ and also that $N^+(p) = N(p)/N^-(p)$ (cf. Eq. (43)), the I -integral is written by Cauchy's theorem as

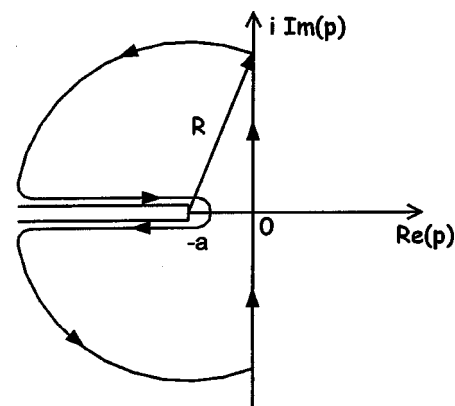


Fig. 7 Contour integration for the evaluation of the complex integral in Eq. (66)

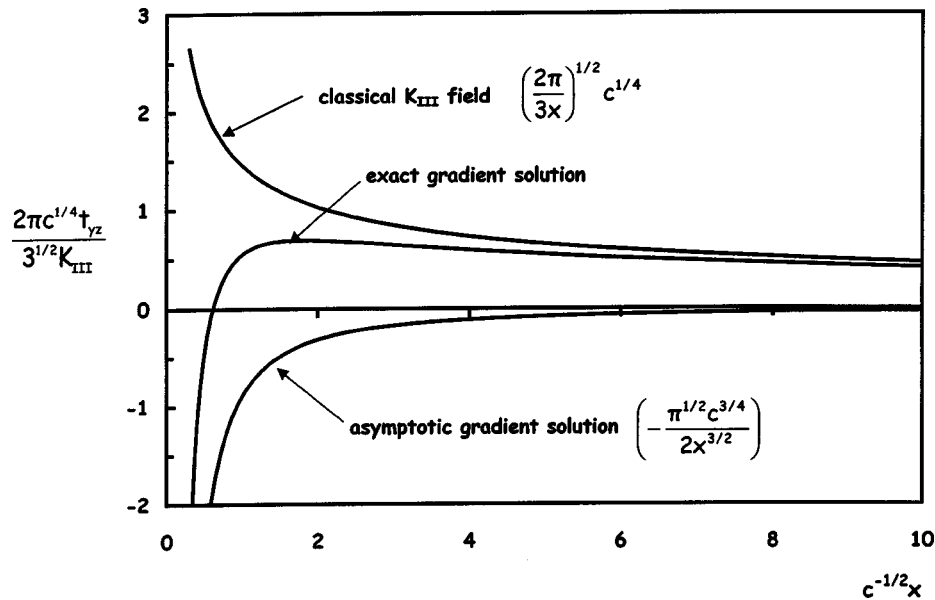


Fig. 8 Graphs of the exact gradient (total monopolar stress), asymptotic gradient (total monopolar stress), and classical K_{III} field solutions in normalized forms

$$\begin{aligned} \frac{1}{2\pi i} I = & -\frac{1}{2\pi i} \left\{ i \int_{\pi/2}^{\pi} R^{3/2} \exp\left(i \frac{3\varphi}{2} - ax + Rxe^{i\varphi}\right) d\varphi \right. \\ & + i \int_{-\infty}^{-a} N^+(p) \cdot (|a+p|)^{1/2} e^{px} dp \\ & + \int_{-a}^0 \frac{[\operatorname{Re} N(p) - i \operatorname{Im} N(p)] (|a+p|)^{1/2} e^{px}}{N^-(p)} dp \\ & + \int_0^{-a} \frac{[\operatorname{Re} N(p) + i \operatorname{Im} N(p)] (|a+p|)^{1/2} e^{px}}{N^-(p)} dp \\ & - i \int_{-a}^{-\infty} N^+(p) \cdot (|a+p|)^{1/2} e^{px} dp + i \int_{-\pi}^{-\pi/2} R^{3/2} \\ & \left. \times \exp\left(i \frac{3\varphi}{2} - ax + Rxe^{i\varphi}\right) d\varphi \right\}, \quad (67) \end{aligned}$$

where R is the radius of the two quarter-circular paths having a center at the point $p = -a$ (see Fig. 7) and the angle φ is defined by the relation $p + a = R \cdot \exp(i\varphi)$. Also, $R \rightarrow \infty$ in the left half-plane, and $\operatorname{Re} N(p) = 2cp^2/3$ and $\operatorname{Im} N(p) = 2(1 - cp^2)(a^2 - p^2)^{1/2} [3|p|]^{-1}$ for p real and $|p| \leq a$. Further, it can be shown

$$\begin{aligned} \frac{1}{2\pi i} I = & \frac{1}{\pi} \left\{ \int_0^a \frac{[\operatorname{Im} N(p)] (a-p)^{1/2} e^{-px}}{N^+(p)} dx \right. \\ & - \int_a^{\infty} N^-(p) \cdot (p-a)^{1/2} e^{-px} dp + R^{3/2} e^{-ax} \\ & \left. \times \int_{\pi/2}^{\pi} \exp(Rx \cdot \cos \varphi) \cdot \cos\left(\frac{3\varphi}{2} + Rx \cdot \sin \varphi\right) d\varphi \right\}. \quad (68) \end{aligned}$$

The third integral inside the braces vanishes as $R \rightarrow \infty$ and it is interesting to note that although the conditions for Jordan's lemma are not met by the integrand in (66), the contribution of the quarter-circular paths is zero because of the existence of the

branch cut for the function $(a+p)^{1/2}$. Therefore, the total monopolar stress ahead of the crack tip is found from the following expression involving two real integrals:

$$\begin{aligned} t_{yz}(x, y=0) = & \frac{K_{III}(3c)^{1/2}}{2\pi} \left\{ \int_0^a \frac{[\operatorname{Im} N(p)] (a-p)^{1/2} e^{-px}}{N^+(p)} dx \right. \\ & \left. - \int_a^{\infty} N^-(p) \cdot (p-a)^{1/2} e^{-px} dp \right\}. \quad (69) \end{aligned}$$

It can be checked that both integrals are convergent. Also, a numerical evaluation of these integrals can easily be accomplished. Finally, the above expression can be written in a more convenient dimensionless form as

$$\begin{aligned} t_{yz}(x, y=0) = & \frac{K_{III} 3^{1/2}}{2\pi c^{1/4}} \left\{ \int_0^1 \frac{[\operatorname{Im} N(p)] (1-p)^{1/2} \exp(-c^{1/2}xp)}{N^+(p)} dp \right. \\ & \left. - \int_1^{\infty} N^-(p) \cdot (p-1)^{1/2} \exp(-c^{1/2}xp) dp \right\}, \quad (70) \end{aligned}$$

where

$$\begin{aligned} N^{\pm}(p) = & \exp\left\{ \frac{1}{\pi} \int_0^1 \arctan\left[\frac{(1-\xi^2)^{3/2}}{\xi^3}\right] \frac{1}{\xi \pm p} d\xi \right\}, \quad (71) \\ \operatorname{Im} N(p) = & \frac{2(1-p^2)^{3/2}}{3p} \quad \text{for } 0 \leq p \leq 1. \quad (72) \end{aligned}$$

The graph of the exact gradient expression for the total monopolar stress ahead of the crack tip in the normalized form $(2\pi c^{1/4} t_{yz} / 3^{1/2} K_{III})$ versus $c^{-1/2}x$ is given in Fig. 8. In the same figure the normalized graphs of the asymptotic gradient solution $(-\pi^{1/2} c^{3/4} / 2x^{3/2})$ and the classical K_{III} field solution $(2\pi/3x)^{1/2} c^{1/4}$ versus $c^{-1/2}x$ are also shown. The latter two graphs are provided for the purpose of comparison with the exact gradient stress distribution. Also, Fig. 9 presents the variation of the exact stress, in the normalized form $(2\pi t_{yz} / (3c)^{1/2} K_{III})$ with (x/h) , where $2h$ is the size of the unit cell of the structured material (intrinsic material length—see Section 2). The two

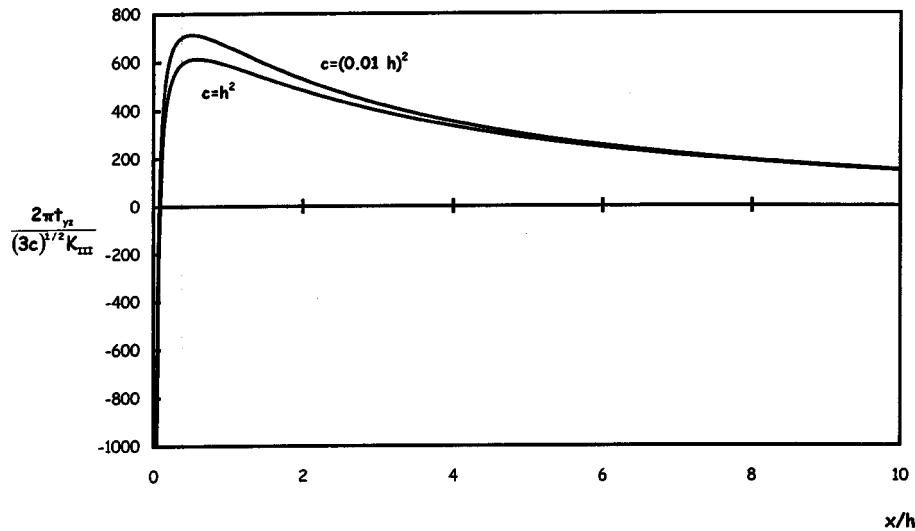


Fig. 9 Variation of the exact total monopolar stress (according to the gradient theory) with (x/h) for the cases $c=h^2$ and $c=(0.01h)^2$. The graphs depict that the cohesive zone is small as compared to the intrinsic material length h and that the stress ahead of the cohesive zone exhibits a bounded maximum.

graphs of Fig. 9 were obtained for the relations $c=(0.01h)^2$ and $c=h^2$. As mentioned in the Introduction, the study by Georgiadis et al. [22] gives the estimate $c=(0.1h)^2$. Thus, in the latter case the stress graph will be in between the two graphs of Fig. 9. The purpose of presenting these two graphs is to make apparent the *bounds* of the region ahead of the tip at which the stress takes on negative values for possible relations between the gradient coefficient c and the intrinsic length h .

On Fig. 8 now, an immediate observation is that the asymptotic gradient solution is inaccurate except for the region very near to the crack tip. Another observation is that the exact gradient stress-field tends to the classical K_{III} stress field at points lying outside the domain where the effects of microstructure are pronounced, i.e., for $x \gg c^{1/2}$. However, in the near-tip region where the distance from the crack-tip is comparable to the length $c^{1/2}$, the two fields differ radically indicating therefore that material microstructure is a significant factor in the fracture behavior of solids. The behavior of the exact solution depicted in Fig. 8 reminds somehow typical *boundary layer* behavior as, e.g., that found for the surface pressure near the leading edge of a Joukowski airfoil (Van Dyke [43]). In particular, the following remarks deserve more attention. For $x < 0.5c^{1/2}$, the stress $t_{yz}(x > 0, y = 0)$ takes on negative values exhibiting therefore a *cohesive-traction* character along the prospective fracture zone (see, e.g., [51,52] for the nature of fracture cohesive zones). However, in view of the relation between c and h , the length L_c (cohesive-zone length of the order of $0.5c^{1/2}$) along which $t_{yz} < 0$ is *extremely* small. For instance, even if h is rather large, say $h = 2 \times 10^{-4}$ m (case of a geomaterial—see [13]), for $c = (0.1h)^2$ we have $L_c = 0.05h = 10^{-5}$ m. The same conclusion can also be reached by observing the graphs of Fig. 9 which show that L_c is a very small fraction of h . It is also interesting to note that L_c does not vary appreciably although c varies over a wide range, i.e., from $c = (0.01h)^2$ to $c = h^2$. Therefore, the length L_c can be considered practically equal to zero and be ignored. Accordingly, the domain of dominance of the $x^{-3/2}$ -singularity being of extremely small size can be considered of no physical importance. Instead, one may attribute physical importance to the solution outside the cohesive zone, where the stress exhibits a maximum that is *bounded*. This maximum may serve as a measure of the critical stress level at which further advancement of the crack may occur. In other words, this result of the present gradient formulation of the crack problem permits a

simple statement of the fracture criterion. Of course, the classical fracture mechanics analysis does not possess this feature since the stress maximum is unbounded at the crack-tip position $x=0$ and the stress drops monotonically for $x > 0$ with no any *local* maximum. Finally, outside the cohesive zone, the stress $t_{yz}(x > L_c, y = 0)$ predicted by the gradient theory is lower than that predicted by the classical elasticity theory.

8 Dynamical Time-Harmonic Mode III Crack Problem

We consider again the semi-infinite crack configuration of Section 4 but now assume a dynamical antiplane shear state. The transient problem leads to an extremely difficult mathematical initial/boundary value problem. Here, as a first step we deal with the *time-harmonic* inertial crack problem which, to our knowledge, consists the first attempt to analyze a dynamical crack problem within gradient elasticity. The more general transient solution may follow from the present one through Fourier synthesis. It is also expected that the basic *spatial* behavior of the solution (e.g., the order of singularities and the near-tip behavior) will be retained in the transient case as well. Within classical elasticity, problems involving cracks under remotely applied time-harmonic loading have been considered by, among others, Cherepanov [53] and Freund [54].

The cracked body is subjected to a remotely applied time-harmonic loading and the crack faces are traction-free. In view of the general expressions given in Section 2, Eqs. (12)–(14) remain the same but (11) and (15)–(17) are replaced by

$$u_x = u_y = 0, \quad (73a)$$

$$u_z \equiv w \neq 0, \quad (73b)$$

$$w \equiv w(x, y, t) = w(x, y) \cdot \exp(i\Omega t), \quad (73c)$$

$$\begin{aligned} \frac{\partial}{\partial x} \left(\tau_{xz} - \frac{\partial m_{xxz}}{\partial x} - \frac{\partial m_{yxz}}{\partial y} \right) + \frac{\partial}{\partial y} \left(\tau_{yz} - \frac{\partial m_{xyz}}{\partial x} - \frac{\partial m_{yyz}}{\partial y} \right) \\ = \rho \frac{\partial^2 w}{\partial t^2} - \frac{\rho h^2}{3} \nabla^2 \left(\frac{\partial^2 w}{\partial t^2} \right), \end{aligned} \quad (74)$$

$$c \nabla^4 w - g \nabla^2 w - k^2 w = 0, \quad (75)$$

$$\sigma_{xz} = \mu g \frac{\partial w}{\partial x} - \mu c \nabla^2 \left(\frac{\partial w}{\partial x} \right), \quad (76a)$$

$$\sigma_{yz} = \mu g \frac{\partial w}{\partial y} - \mu c \nabla^2 \left(\frac{\partial w}{\partial y} \right), \quad (76b)$$

where Ω is the frequency of the time-harmonic state, $g = (1 - \Omega^2(\rho h^2/3\mu))$, and $k = (\Omega/V)$ with $V = (\mu/\rho)^{1/2}$ being the shear-wave velocity in the absence of gradient effects (i.e., in classical elasticity). Equation (75) is the field equation of the problem. It is called metaharmonic and appears also in the problem of bending vibrations of thin plates (Vekua [55]). More details about it can be found in [13,20]. In what follows, as is standard in time-harmonic problems, it is understood that all field quantities are to be multiplied by the factor $\exp(i\Omega t)$ and that the real part of the resulting expression is to be taken.

The above equations are also supplied by the boundary conditions (18)–(21). The resulting boundary value problem is attacked again by the Wiener-Hopf method. First, transforming (75) with (30a) gives the ordinary differential equation

$$c \frac{d^4 w^*}{dy^4} + (2cp^2 - g) \frac{d^2 w^*}{dy^2} + (cp^4 - gp^2 - k^2)w^* = 0, \quad (77)$$

with the following general solution (bounded as $y \rightarrow +\infty$)

$$w^*(p, y) = B(p) \cdot \exp(-\bar{\beta}y) + C(p) \cdot \exp(-\bar{\gamma}y) \quad \text{for } y \geq 0, \quad (78)$$

where

$$\bar{\beta} \equiv \bar{\beta}(p) = i(p^2 + \sigma^2)^{1/2} \quad (79a)$$

with

$$\sigma = \frac{[(g^2 + 4ck^2)^{1/2} - g]^{1/2}}{(2c)^{1/2}} > 0, \quad (79b)$$

$$\bar{\gamma} \equiv \bar{\gamma}(p) = (\tau^2 - p^2)^{1/2} \quad (80a)$$

with

$$\tau = \frac{[(g^2 + 4ck^2)^{1/2} + g]^{1/2}}{(2c)^{1/2}} > 0. \quad (80b)$$

In the above equations, $B(p)$ and $C(p)$ are unknown functions, and the complex p -plane should be cut in the way shown in Fig. 10. Finally, the Laplace-transformed stresses that enter the boundary conditions are found to be

$$\sigma_{yz}^*(p, y) = -\mu c (\tau^2 B \bar{\beta} e^{-\bar{\beta}y} - \sigma^2 C \bar{\gamma} e^{-\bar{\gamma}y}), \quad (81)$$

$$m_{yyz}^*(p, y) = \mu c (B \bar{\beta}^2 e^{-\bar{\beta}y} + C \bar{\gamma}^2 e^{-\bar{\gamma}y}), \quad (82)$$

$$m_{yxz}^*(p, y) = -\mu c p (B \bar{\beta} e^{-\bar{\beta}y} + C \bar{\gamma} e^{-\bar{\gamma}y}). \quad (83)$$

Next, to formulate the Wiener-Hopf equation, the same “half-line” transforms are defined as in (36) and (37). Also, (38) and (39) apply in the present case too. The usual procedure of eliminating the functions (B, C) in the system of equations resulting from the transformed boundary conditions leads then to the following Wiener-Hopf equation

$$T^+(p) = \frac{\mu c}{\chi^2} \bar{\beta} \bar{\gamma} (\bar{\beta}^3 - \bar{\gamma}^3) \cdot W^-(p), \quad (84)$$

where $\chi^2 = (g^2 + 4ck^2)^{1/2}/c$ is a positive real constant dependent upon the material properties and the frequency. Notice also that $\chi^2 = (\sigma^2 + \tau^2) = \bar{\gamma}^2 - \bar{\beta}^2$.

Further, since a product factorization of the function $\bar{\gamma}$ is immediately accomplished by inspection as $\bar{\gamma}(p) = (\tau + p)^{1/2}(\tau - p)^{1/2}$, Eq. (84) takes the form

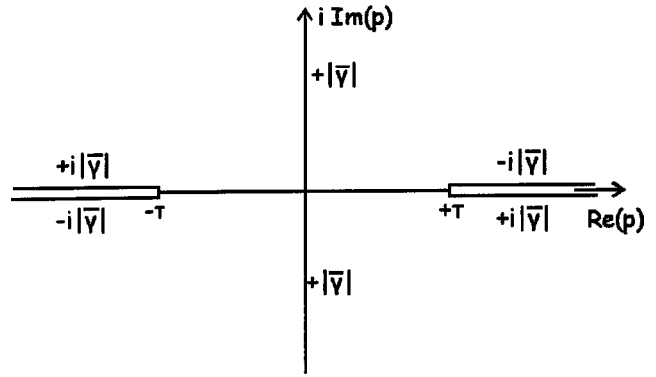
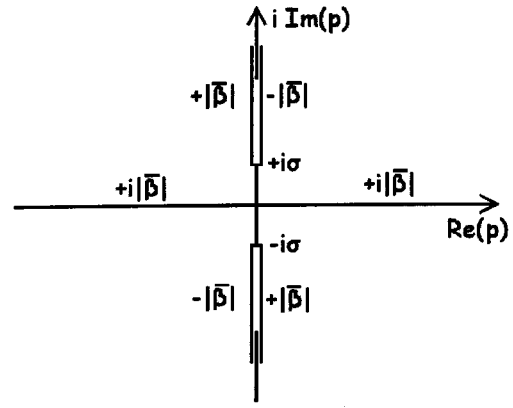


Fig. 10 Branch cuts for the functions $(\bar{\beta}, \bar{\gamma})$

$$\frac{T^+(p)}{(\tau + p)^{1/2}} = -\frac{\mu c}{\chi^2} (\tau - p)^{1/2} (\sigma^2 + p^2) \cdot \bar{L}(p) \cdot W^-(p), \quad (85)$$

where the kernel function $\bar{L}(p)$ is given as

$$\bar{L}(p) = (\sigma^2 + p^2) + \frac{(\tau^2 - p^2)^{3/2}}{i(\sigma^2 + p^2)^{1/2}}. \quad (86)$$

Now, contrary to the static case analyzed in Section 6, the kernel function in the present dynamic case exhibits two zeros in the complex plane. This was found through a rather involved procedure using the principle of the argument, [37], and taking care of the behavior and the branch cuts of the functions $(\bar{\beta}, \bar{\gamma})$. In addition, a check was made by the symbolic program MATHEMATICA™. Thus, the function $\bar{L}(p)$ exhibits the (non-extraneous) zeros

$$\pm Z = \pm \left\{ \frac{g}{2c} + i \left[\frac{(g^2/4c^2) + (k^2/c)}{3} \right]^{1/2} \right\}^{1/2}, \quad (87)$$

and, in addition, has the asymptotic behavior $\lim_{|p| \rightarrow \infty} \bar{L}(p) \rightarrow 3\chi^2/2$. Next, the function $M(p)$ is introduced as

$$M(p) = \frac{2}{3\chi^2} \frac{(\tau^2 - p^2) \cdot \bar{L}(p)}{p^2 - Z^2}, \quad (88)$$

which no longer exhibits zeros and also has the desired asymptotic property $\lim_{|p| \rightarrow \infty} M(p) \rightarrow 1$. This new form of the kernel permits its product factorization through Cauchy's integral theorem.

In view of the above, the Wiener-Hopf equation of the problem becomes

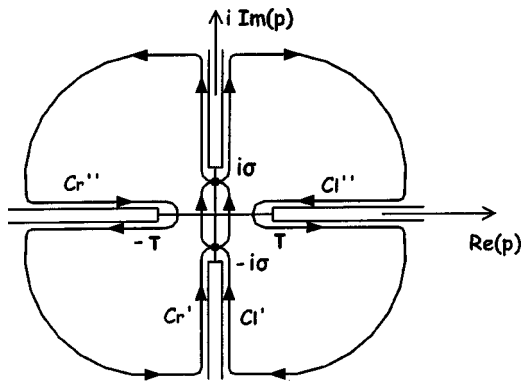


Fig. 11 Contour integrations for the factorization of the kernel function defined in Eq. (88)

$$\frac{T^+(p) \cdot (\tau + p)^{1/2}}{(p + Z)} = -\frac{3\mu c}{2} \frac{(\sigma^2 + p^2)(p - Z)}{(\tau - p)^{1/2}} M(p) \cdot W^-(p), \quad (89)$$

and the kernel is written as the following product of two analytic and nonzero functions defined in pertinent half-plane domains of the complex plane

$$M(p) = M^+(p) \cdot M^-(p), \quad (90)$$

where

$$M^+(p) = \exp\left\{-\frac{1}{2\pi i} \int_{C_l' + C_l''} \frac{\ln[M(\zeta)]}{\zeta - p} d\zeta\right\}, \quad (91a)$$

$$M^-(p) = \exp\left\{\frac{1}{2\pi i} \int_{C_r' + C_r''} \frac{\ln[M(\zeta)]}{\zeta - p} d\zeta\right\}. \quad (91b)$$

The use of Cauchy's integral theorem to accomplish (90) is depicted in Fig. 11. Notice that Cauchy's theorem still applies in this case of a *nonsimple* contour (a contour with self-intersections) because the number of intersections is finite (see for the general result in, e.g., Ablowitz and Fokas [56]). $M^+(p)$ is analytic and nonzero in $\text{Re}(p) > 0$ and $M^-(p)$ is analytic and nonzero in $\text{Re}(p) < 0$. The integration path ($C_l' + C_l''$) begins from the point Σ at $(-i\sigma + i\varepsilon)$, with ε real such $\varepsilon \rightarrow +0$, and runs along the entire imaginary axis (along the two cuts, it runs parallel to them on the right) and around the cut along the positive real axis. The integration path ($C_r' + C_r''$) begins from the point Σ , it runs along the entire imaginary axis (along the two cuts, it runs parallel to them on the left) and around the cut along the negative real axis. Both integration paths end at the point Σ , and the second path is considered a continuation of the first so that Cauchy's theorem is applied and (90) is obtained. In both cases, the quarter-circular paths at infinity have a zero contribution according to Jordan's lemma. Finally, the small semi-circular paths around the branch points have a zero contribution.

Then, with the formal product factorization in hand, Eq. (89) is written under the following form that defines a function $\bar{E}(p)$:

$$\frac{T^+(p) \cdot (\tau + p)^{1/2}}{(p + Z) \cdot M^+(p)} = -\frac{3\mu c}{2} \frac{(\sigma^2 + p^2)(p - Z)}{(\tau - p)^{1/2}} M^-(p) \cdot W^-(p) \equiv \bar{E}(p). \quad (92)$$

The above equation strictly holds along the segment of the imaginary axis ($\text{Re}(p) = 0, -\sigma < \text{Im}(p) < \sigma$) and $\bar{E}(p)$ is therefore defined only along this segment. This restriction of the validity of the Wiener-Hopf equation to a *finite* segment only (notice that in the static case treated before and invariably in crack problems within classical elasticity—both static and dynamic—the Wiener-Hopf equation holds along an infinite line or strip) is another

novel feature of the present mathematical problem. Still, the theorem of analytic continuation applies and leads us to conclude that $\bar{E}(p)$ is an entire function. Working also along the same lines as those in the respective analysis of the previous static case, we find that the near-tip stress and displacement fields behave as in (51). Results analogous to the ones in the static case can be further obtained from the basic analysis of this section.

9 Conclusions

The present work was concerned with the exact determination of mode III crack-tip fields in a microstructured body under a remotely applied loading. The material microstructure was modeled according to the Mindlin-Green-Rivlin theory of generalized elastic continua (dipolar gradient or strain-gradient theory of grade two). A simple but yet rigorous version of this theory was employed by considering an isotropic linear expression of the elastic strain-energy density in antiplane shearing that involves only two material constants (the shear modulus and the gradient coefficient). The formulation of the problem and the solution methods were exact. The boundary value problem was attacked by the Wiener-Hopf technique but the asymptotic Williams technique was also employed in a preliminary analysis. Both static and time-harmonic dynamic analyses were provided. A singular-perturbation character was exhibited within the gradient formulation and the concept of a boundary layer was employed.

The results for the near-tip field showed significant departure from the predictions of the classical fracture mechanics. In particular, it was found that cohesive stresses develop in the immediate vicinity of the crack tip and that, ahead of the small cohesive zone, the stress distribution exhibits a local maximum that is bounded. This maximum value may serve, therefore, as a measure of the critical stress level at which further advancement of the crack may occur. In addition, the crack-face displacement closes more smoothly, in the vicinity of the crack tip, as compared to the classical result. The new formulation of the crack problem required also new extended definitions for the J -integral and the energy release rate. The determination of these quantities was made possible through the use of the theory of generalized functions.

A final notice pertains to the possibility of generalizing the present analysis by considering a continuum theory of even higher order than that of dipolar gradient theory. The next step could be a tripolar theory. The dipolar theory involves doublets of forces (double forces) as "internal" forces. The tripolar theory will involve rather doublets of moments (triple forces). Besides the fact that the latter generalized forces possess a not so clear physical meaning, the increased complexity of such a theory does not hold much hope for treating practical problems.

Acknowledgments

The author is thankful to Prof. L.M. Brock (University of Kentucky) for discussions on aspects of the mathematical analysis contained in this work. Also, the author is thankful to Prof. I. Vardoulakis (NTU Athens) and N. Aravas (University of Thessaly) for discussions on generalized continuum theories. Financial support of this work under the "Thales" program of the NTUA is gratefully acknowledged.

References

- [1] Mindlin, R. D., 1964, "Micro-Structure in Linear Elasticity," *Arch. Ration. Mech. Anal.*, **16**, pp. 51–78.
- [2] Green, A. E., and Rivlin, R. S., 1964, "Multipolar Continuum Mechanics," *Arch. Ration. Mech. Anal.*, **17**, pp. 113–147.
- [3] Green, A. E., 1965, "Micro-Materials and Multipolar Continuum Mechanics," *Int. J. Eng. Sci.*, **3**, pp. 533–537.
- [4] Mindlin, R. D., and Eshel, N. N., 1968, "On First Strain-Gradient Theories in Linear Elasticity," *Int. J. Solids Struct.*, **4**, pp. 109–124.
- [5] Weitsman, Y., 1966, "Strain-Gradient Effects Around Cylindrical Inclusions and Cavities in a Field of Cylindrically Symmetric Tension," *ASME J. Appl. Mech.*, **33**, pp. 57–67.

- [6] Day, F. D., and Weitsman, Y., 1966, "Strain-Gradient Effects in Microlayers," *ASCE J. Eng. Mech.*, **92**, pp. 67–86.
- [7] Cook, T. S., and Weitsman, Y., 1966, "Strain-Gradient Effects around Spherical Inclusions and Cavities," *Int. J. Solids Struct.*, **2**, pp. 393–406.
- [8] Herrmann, G., and Achenbach, J. D., 1968, "Applications of Theories of Generalized Cosserat Continua to the Dynamics of Composite Materials," *Mechanics of Generalized Continua*, E. Kroener, ed., Springer, Berlin, pp. 69–79.
- [9] Achenbach, J. D., Sun, C. T., and Herrmann, G., 1968, "On the Vibrations of a Laminated Body," *ASME J. Appl. Mech.*, **35**, pp. 689–696.
- [10] Vardoulakis, I., and Sulem, J., 1995, *Bifurcation Analysis in Geomechanics*, Blackie Academic and Professional (Chapman and Hall), London.
- [11] Fleck, N. A., Muller, G. M., Ashby, M. F., and Hutchinson, J. W., 1994, "Strain Gradient Plasticity: Theory and Experiment," *Acta Metall. Mater.*, **42**, pp. 475–487.
- [12] Lakes, L., 1995, "Experimental Methods for Study of Cosserat Elastic Solids and Other Generalized Elastic Continua," *Continuum Models for Materials with Microstructure*, H.-B. Muhlhause, ed., John Wiley and Sons, Chichester, pp. 1–25.
- [13] Vardoulakis, I., and Georgiadis, H. G., 1997, "SH Surface Waves in a Homogeneous Gradient Elastic Half-Space with Surface Energy," *J. Elast.*, **47**, pp. 147–165.
- [14] Wei, Y., and Hutchinson, J. W., 1997, "Steady-State Crack Growth and Work of Fracture for Solids Characterized by Strain Gradient Plasticity," *J. Mech. Phys. Solids*, **45**, pp. 1253–1273.
- [15] Begley, M. R., and Hutchinson, J. W., 1998, "The Mechanics of Size-Dependent Indentation," *J. Mech. Phys. Solids*, **46**, pp. 2049–2068.
- [16] Exadaktylos, G., and Vardoulakis, I., 1998, "Surface Instability in Gradient Elasticity With Surface Energy," *Int. J. Solids Struct.*, **35**, pp. 2251–2281.
- [17] Huang, Y., Zhang, L., Guo, T. F., and Hwang, K. C., 1997, "Near-Tip Fields for Cracks in Materials With Gradient Effects," *Proceedings of the IUTAM Symposium on Nonlinear Analysis of Fracture*, J. R. Willis, ed., Kluwer Academic Publishers, Dordrecht, pp. 231–243.
- [18] Zhang, L., Huang, Y., Chen, J. Y., and Hwang, K. C., 1998, "The Mode-III Full-Field Solution in Elastic Materials With Strain Gradient Effects," *Int. J. Fract.*, **92**, pp. 325–348.
- [19] Chen, J. Y., Huang, Y., and Ortiz, M., 1998, "Fracture Analysis of Cellular Materials: A Strain Gradient Model," *J. Mech. Phys. Solids*, **46**, pp. 789–828.
- [20] Georgiadis, H. G., and Vardoulakis, I., 1998, "Anti-Plane Shear Lamb's Problem Treated by Gradient Elasticity With Surface Energy," *Wave Motion*, **28**, pp. 353–366.
- [21] Georgiadis, H. G., Vardoulakis, I., and Lykotrifitis, G., 2000, "Torsional Surface Waves in a Gradient-Elastic Half-Space," *Wave Motion*, **31**, pp. 333–348.
- [22] Georgiadis, H. G., Vardoulakis, I., and Velgaki, E. G., 2002, "Dispersive Rayleigh-Wave Propagation in Microstructured Solids Characterized by Dipolar Gradient Elasticity," *J. Elast.*, submitted for publication.
- [23] Georgiadis, H. G., and Velgaki, E. G., 2002, "High-Frequency Rayleigh Waves in Materials With Microstructure and Couple-Stress Effects," *Int. J. Solids Struct.*, **40**, pp. 2501–2520.
- [24] Amanatidou, E., and Aravas, N., 2001, "Finite Element Techniques for Gradient Elasticity Problems," *Proceedings of the 6th Greek National Congress of Mechanics*, Hellenic Society of Theoretical and Applied Mechanics, **2**, pp. 149–154.
- [25] Gazis, D. C., Herman, R., and Wallis, R. F., 1960, "Surface Elastic Waves in Cubic Crystals," *Phys. Rev.*, **119**, pp. 533–544.
- [26] Jaunzemis, W., 1967, *Continuum Mechanics*, MacMillan, New York.
- [27] Fung, Y. C., 1965, *Foundations of Solid Mechanics*, Prentice-Hall, Englewood Cliffs, NJ.
- [28] Ignaczak, J., 1971, "Tensorial Equations of Motion for Elastic Materials With Microstructure," *Trends in Elasticity and Thermoelasticity* (W. Nowacki Anniversary Volume), Wolters-Noordhoff, Groningen, pp. 89–111.
- [29] Rice, J. R., 1968, "A Path Independent Integral and the Approximate Analysis of Strain Concentration by Notches and Cracks," *ASME J. Appl. Mech.*, **35**, pp. 379–386.
- [30] Rice, J. R., 1968, "Mathematical Analysis in the Mechanics of Fracture," *Fracture*, H. Liebowitz, ed., **2**, Academic Press, New York, pp. 191–311.
- [31] Atkinson, C., and Leppington, F. G., 1974, "Some Calculations of the Energy-Release Rate G for Cracks in Micropolar and Couple-Stress Elastic Media," *Int. J. Fract.*, **10**, pp. 599–602.
- [32] Lubarda, V. A., and Markenscoff, X., 2000, "Conservation Integrals in Couple Stress Elasticity," *J. Mech. Phys. Solids*, **48**, pp. 553–564.
- [33] Williams, M. L., 1952, "Stress Singularities Resulting from Various Boundary Conditions in Angular Corners of Plates in Extension," *ASME J. Appl. Mech.*, **74**, pp. 526–528.
- [34] Williams, M. L., 1957, "On the Stress Distribution at the Base of a Stationary Crack," *ASME J. Appl. Mech.*, **79**, pp. 109–114.
- [35] Barber, J. R., 1992, *Elasticity*, Kluwer Academic Publishers, Dordrecht.
- [36] van der Pol, B., and Bremmer, H., 1950, *Operational Calculus Based on the Two-Sided Laplace Integral*, Cambridge University Press, Cambridge, UK.
- [37] Carrier, G. A., Krook, M., and Pearson, C. E., 1966, *Functions of a Complex Variable*, McGraw-Hill, New York.
- [38] Roos, B. W., 1969, *Analytic Functions and Distributions in Physics and Engineering*, John Wiley and Sons, New York.
- [39] Mitra, R., and Lee, S. W., 1971, *Analytical Techniques in the Theory of Guided Waves*, MacMillan, New York.
- [40] Gel'fand, I. M., and Shilov, G. E., 1964, *Generalized Functions*, **1**, Academic Press, New York.
- [41] Lauwerier, H. A., 1963, "The Hilbert Problem for Generalized Functions," *Arch. Ration. Mech. Anal.*, **13**, pp. 157–166.
- [42] Knowles, J. K., and Pucik, T. A., 1973, "Uniqueness for Plane Crack Problems in Linear Elastostatics," *J. Elast.*, **3**, pp. 155–160.
- [43] Van Dyke, M., 1964, *Perturbation Methods in Fluid Mechanics*, Academic Press, New York.
- [44] Rice, J. R., 1974, "Limitations to the Small Scale Yielding Approximation for Crack Tip Plasticity," *J. Mech. Phys. Solids*, **22**, pp. 17–26.
- [45] Mills, N. J., 1974, "Dugdale Yielded Zones in Cracked Sheets of Glassy Polymers," *Eng. Fract. Mech.*, **6**, pp. 537–549.
- [46] Elssner, G., Korn, D., and Ruhle, M., 1994, "The Influence of Interface Impurities on Fracture Energy of UHV Diffusion Bonded Metal-Ceramic Bicycstals," *Scr. Metall. Mater.*, **31**, pp. 1037–1042.
- [47] Bogy, D. B., and Sternberg, E., 1967, "The Effect of Couple-Stresses on Singularities due to Discontinuous Loadings," *Int. J. Solids Struct.*, **3**, pp. 757–770.
- [48] Prakash, V., Freund, L. B., and Clifton, R. J., 1992, "Stress Wave Radiation From a Crack Tip During Dynamic Initiation," *ASME J. Appl. Mech.*, **59**, pp. 356–365.
- [49] Fisher, B., 1971, "The Product of Distributions," *Quart. J. Math. Oxford*, **22**, pp. 291–298.
- [50] Bueckner, H. F., 1958, "The Propagation of Cracks and the Energy of Elastic Deformation," *Trans. ASME*, **24**, pp. 1225–1230.
- [51] Barenblatt, G. I., 1962, "The Mathematical Theory of Equilibrium Cracks in Brittle Fracture," *Adv. Appl. Mech.*, **7**, pp. 55–129.
- [52] Nilsson, F., and Stahle, P., 1988, "Crack Growth Criteria and Crack Tip Models," *SM Arch.*, **13**(4), pp. 193–238.
- [53] Cherepanov, G. P., 1979, *Mechanics of Brittle Fracture*, McGraw-Hill, New York.
- [54] Freund, L. B., 1990, *Dynamic Fracture Mechanics*, Cambridge University Press, Cambridge, UK.
- [55] Vekua, I. N., 1968, *New Methods for Solving Elliptic Equations*, North-Holland, Amsterdam.
- [56] Ablowitz, M. J., and Fokas, A. S., 1997, *Complex Variables: Introduction and Applications*, Cambridge University Press, Cambridge, UK.